A Multisensory Approach for Remote Health Monitoring of Older People

Haobo Li, Aman Shrestha, *Student Member, IEEE*, Hadi Heidari, *Senior Member, IEEE*, Julien Le Kernec, *Senior Member, IEEE*, and Francesco Fioranelli, *Member, IEEE*

***Abstract*—Growing life expectancy and increasing incidence of multiple chronic health conditions are significant societal challenges. Different technologies have been proposed to address these issues, detect critical events, such as stroke or falls, and monitor automatically human activities for health condition inference and anomaly detection. This paper aims to investigate two types of sensing technologies proposed for assisted living: wearable and radar sensors. First, different feature selection methods are validated and compared in terms of accuracy and computational loads. Then, information fusion is applied to enhance activity classification accuracy combining the two sensors. Improvements in classification accuracy of approximately 12% using feature level fusion are achieved with both support vector machine s (SVMs) and *k*-nearest neighbor (KNN) classifiers. Decision-level fusion schemes are also investigated, yielding classification accuracy in the order of 97%–98%.**

***Index Terms*—Human activity classification, fall detection, ambient assisted living, inertial sensors, magnetic sensors, radar sensors, multisensory data fusion, feature selection.**

I. Introduction

THE increase in life expectancy has posed new healthcare challenges in recent years. People wish to keep their quality of life and independence for as long as possible. However, living longer is also characterized by an increasing incidence of multiple chronic conditions and critical events such as falls or strokes. These have societal costs in terms of increasing expenditure for health provision, but also obvious consequences on the wellbeing of the older people in our societies and their families [1]–[3]. Evidence from medical studies shows that prompt help and intervention can significantly reduce the negative consequences of critical events (such as falls). Furthermore, it has been shown that subtle changes in the daily activities pattern and behavior may help with the diagnostic of health problems.

Different technologies have been proposed in this context to achieve these two objectives, fall detection [4]–[8] and daily activity monitoring [3]. These include video and depth cameras, acoustic and passive infrared (PIR) sensors, smart floors, inertial sensors such as accelerometers and gyroscopes [5], [9], [10], magnetic sensors, and radio-frequency (RF) sensors that use active or passive radar principles [11]–[15]. Each sensing technology presents advantages and disadvantages inherent to its implementation and in aspects related to the required users' compliance or perception. For example, cameras can provide very high activity classification accuracy, but they may raise privacy objections. Wearable sensors tend to be cost-effective and easily miniaturized, but users may need to remember to wear and use them properly, which can be an issue for older people and people with cognitive impairments [16]. Radar sensors are a relatively new technology in this context, and their effectiveness in realistic scenarios beyond "proof of concept" cases is still being validated [17]. Simple sensors such as PIRs may have a limited detection range and do not provide enough information for fine activity classification.

In this paper, we expand our preliminary work in [18] and present a detailed analysis of feature selection and information fusion methods when using simultaneous information from wearable sensors and radar sensor, for a new dataset comprised of new subjects. Inertial sensors are attractive for their compact form, low cost, relatively simple signal processing, and possibility of embedding into everyday objects such as phones or watches, which users may naturally take with them. Radar sensors are attractive for their contactless and non-cooperative monitoring capabilities, no reliance on users' compliance, and detection/classification ranges of tens of meters. They are expected to be perceived as more privacy-oriented, as no plain images of the monitored people are recorded [19]. The simultaneous use of heterogeneous sensors allows overcoming the performance limitations of each sensor considered individually, or possible malfunctions of one of them (for example "drift problem" inherent to accelerometers [13], or classification accuracy reduction for radar sensors relying on Doppler-based classification for tangential views of the person monitored [17]). This multi-sensory approach could fit well with future realistic scenarios, where a variety of monitoring smart sensors are deployed and used simultaneously in home environments, supported by developments in the Internet of Things and advanced (5G) communications.

Although information fusion for different inertial sensors has been proposed [13], their combination and experimental verification with radar sensing presented here is to the best of our

Manuscript received December 6, 2017; revised February 26, 2018; accepted April 10, 2018. Date of publication April 16, 2018; date of current version May 19, 2018. This work was supported by the EPSRC under Grant "INSHEP" EP/R041679/1. The work of A. Shrestha was supported by the Doctoral Training Award for his Ph.D. degree at the School of Engineering, University of Glasgow. This paper was presented in part at the 2017 IEEE Sensors Conference, Glasgow, U.K., October 2017. *(Corresponding author: Francesco Fioranelli.)*

The authors are with the School of Engineering, University of Glasgow, Glasgow G12 8QQ, U.K. (e-mail: h.li.4@research.gla.ac.uk; a.shrestha.1@research.gla.ac.uk; hadi.heidari@glasgow.ac.uk; Julien.Lekernec@glasgow.ac.uk; francesco.fioranelli@glasgow.ac.uk).

Color versions of one or more of the figures in this paper are available online at http://ieeexplore.ieee.org.

Digital Object Identifier 10.1109/JERM.2018.2827099

knowledge, innovative. Furthermore, fusion approaches classically used for inertial sensors focus on signal level fusion, employing methods such as vector observation, Kalman filtering or other forms of signal filtering [13], whereas in our work, we propose simpler fusion at feature and decision level, combined with effective feature selection approaches.

Compared with the preliminary results presented in [18], this work considers additional features extracted from the wearable and radar sensor data, investigates three different methods to perform feature selection for each of these sensors, and presents different approaches for decision fusion. These include a voting-based system comprised of two support vector machine (SVM) classifiers and two k nearest neighbor (KNN) classifiers, to exploit strengths from different classifiers and sensors in the decision process. The aim is to improve the classification accuracy and minimize false alarms when detecting fall events, the main activity of interest, for which misdetections or false alarms must be avoided.

The paper is organized as follows: Section II describes the data collection, and Section III the extraction of features. Section IV evaluates the classifiers used in this work and the different feature selection methods. Section V presents the methods for decision level fusion and the subsequent improvements in classification accuracy. Finally, conclusions and future work are discussed in Section VI.

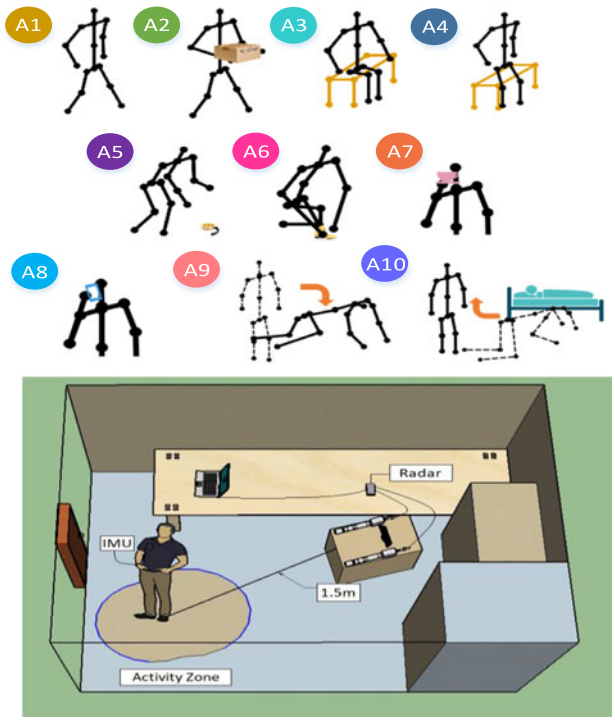

Fig. 1. Simple sketch of the 10 classified activities (top) and experimental setup (bottom).

II. Data Collection and Pre-Processing

Data were collected using a nine degrees of freedom inertial sensor within a smartphone, and a frequency modulated continuous wave radar system. The inertial sensor includes a tri-axial accelerometer, gyroscope, and magnetometer, and is capable of simultaneously recording the acceleration, angular velocity and magnetic-field strength at approximately 100 Hz sampling rate. The radar sensor operates at a carrier frequency of 5.8 GHz, with the transmitted signal having 400 MHz instantaneous bandwidth and 1 ms duration. Transmitted power of the radar is in the order of +19 dBm, with the gain of the transmitting and receiving Yagi antennas approximately equal to 17 dB.

Fig. 1 shows a sketch of the measurement environment (an office room/laboratory for the Communication, Sensing and Imaging group at the University of Glasgow), with the antennas and a processing laptop located on the table near the subject and a token participant in the activity zone. The smartphone was held with a Velcro-strap on the wrist of the participating subject's dominant hand while recording data, whereas the radar system and antennas were placed on a box facing the activity zone. The separation between the antennas was approximately 30 cm (quasi-monostatic setup), and the distance from them to the subjects was approximately 1.5 m. Vertical polarization was used for these measurements.

Ten different activities were recorded as depicted in the top part of Fig. 1, involving nine volunteers aged 23 to 31 years old. The activities were described in our previous work [18]. Three repetitions for each activity for each subject were recorded, generating a set of 270 sample measurements with simultaneous readings from the wearable sensor, the radar sensor, as well as a Microsoft Kinect recording for ground truth.

Although not large, the number of selected subjects and activities is still significant when compared to other studies published in this field, such as the review presented in [13] (where only 14% of the 37 studies reviewed on wearables considered more than 10 subjects). Variety in the forms of gender (two participants were female), body shapes and dominant hand (participants with both left and right dominant hands) are also present in our dataset, making it more representative than others analyzed in other papers (for example, [8] had only three male subjects). Furthermore, the experiment is designed to include deliberately "confusers", that is activities that can be similar to fall events – such as sitting and bending down, which have a strong acceleration component towards the floor. There are also activities that are similar in pairs, such as 'walking' A1 and 'moving object' A2, or 'drinking' A7 and 'taking a call' A8 in Fig. 1. This is intended to help test the robustness of the proposed classification methods, with respect to "fall" A9, the main class of interest.

Prior to data analysis, the signals collected by the wearable sensor were pre-processed through a Chebyshev-II band-pass filter [12], [14] to remove undesired noise and components, for example those generated by small vibrations of the device. For radar, the micro-Doppler effect [21] is visible within the spectrograms. These are Doppler versus time plots where the movements of torso, limbs, and other body parts generate a distinctive pattern; some examples are shown in [22]. To generate the spectrogram, short-time Fourier transform of the radar data with a window of 0.2 s and 95% overlap were taken to characterise the time variant Doppler shifts associated with the

TABLE I
FEATURES EXTRACTED FROM THE INERTIAL SENSOR IN TIME AND FREQUENCY DOMAINS (*IDENTIFIES SALIENT FEATURES)

Time domain	#	Frequency domain	#
Mean	3	Spectral Power*	9
Standard Deviation	3	Coefficients Sum*	3
Autocorrelation(Mean,STD*)	6	Spectral Entropy	3
Cross Correlation(Mean*,STD*)	6		
Variance	3		
RMS* (Root Mean Square)	3		
MAD (Median Absolute Deviation)	3		
Inter-quadrature Range	3		
Range	3		
Minimum*	3		
25th percentiles	3		
75th percentiles	3		
Skewness	3		
Kurtosis	3		
Number of features	**48**	**Number of features**	**15**

TABLE II
FEATURES EXTRACTED FROM SPECTROGRAMS OBTAINED WITH THE RADAR SENSOR (*IDENTIFIES SALIENT FEATURES)

Feature Category	Radar Features	#
Textural	Entropy of spectrogram	1
	Skewness of spectrogram	1
Physical	Centroid of spectrogram (mean & variance)*	2
	Bandwidth of spectrogram (mean & variance)*	2
	Energy curve of spectrogram*	3
Transform based	Singular Value Decomposition (mean & variance of right and left vectors)*	13
	Range Doppler velocity	1
	Range Doppler displacement	1
	Range Doppler dispersion	1
	Energy curve of spectrogram*	3
	Step repetition frequency	1
	Step repetition frequency band peak	*2*
	Number of features	**28**

movement of different body parts. Prior to this, moving target indicator filtering was performed to remove static targets from the spectrograms, i.e., strong reflections from the static environment (walls, furniture).

III. FEATURE EXTRACTION

Numerical parameters referred to as features were extracted from the pre-processed data of each sensor. For the IMU, 177 features were extracted from the tri-axial sensors: 63 for the accelerometer, 57 for the gyroscope, and 57 for the magnetometer respectively. Features generated are the same for each sensor except for skewness and kurtosis, which are exclusive to the accelerometer. These features were inspired by previous work in the literature [23]–[25] and summarised in Table I where they are divided into time and frequency domains. Time domain features include raw signal mean; raw signal variance, which evaluates the samples dispersion around their mean value; higher statistical moments (skewness and kurtosis), and correlation coefficients which identify activities with commensurate movements in different axis. Frequency domain features aim to capture the spectral energy distribution, they include amplitude of the power spectral density; the sum of Fourier transform coefficients, and the spectral entropy based on power spectrum [25].

Different features have been suggested in the literature for classification with radar [22], [26], and these features, listed in Table II, can be grouped into three categories: Physical, Transform domain, and Textural.

Physical features are directly related to the kinematics of the movement represented in the spectrograms. Main features utilised from this subcategory are centroid, which represents the localised centre of gravity of the micro-Doppler signature and bandwidth, which is the derived Doppler spread. Both of these features have been widely used in classification applications [25] and are robust features in this area. Transform domains represent the projection of the spectrogram to alternate domains for feature. Cadence velocity diagram exploits time varying information in the instantaneous frequency of a spectrogram [28], whereas singular value decomposition (SVD) preserves the information content of the signal by projecting the spectrogram into spectral and temporal domains [29], [30]. Step repetition frequency is derived from the cadence velocity diagram [31] whereas for the SVD moments of the first few vectors of the left and right singular vectors respectively, are used. Textural features are inspired by classical feature extraction from image recognition. Entropy of the grey level histogram of an image equates to the average information within an image, and skewness of the histogram indicates energy level shifts [32].

The following sections will describe how these features are used as classifier inputs for monitoring activities, and how less informative features can be deselected to improve the classification performance and reduce computational cost.

TABLE III
COMPARISON OF CLASSIFICATION ACCURACY BETWEEN SENSORS

Classification Accuracy (%)	SVM	KNN
Accelerometer	85.2	79.6
Gyroscope	84.1	79.6
Magnetometer	80.4	69.6
Inertial	89.3	85.2
Radar	77.9	70.7

IV. CLASSIFICATION AND FEATURE SELECTION

A. Classification Methods

For classification, an SVM with a quadratic kernel and a KNN with $K = 10$ were used to discriminate between the activities. A description of the classifiers is available in [33], [34]. The classifiers were trained and validated using k-folds as follows: the feature set was partitioned into 10 "folds" randomly, nine folds were used to train the classifiers with the last fold being the test set. This is performed until every fold has been tested against, and the validation accuracy is averaged over the 10 folds.

Results for the classification accuracy when using all the available features for KNN and SVM are summarized in Table III for each sensor, where accelerometer and gyroscope produce similar results, while magnetometer and radar are below by approximately 4% and 6.1% with SVM. Furthermore, the

results of magnetometer and radar are significantly lower with KNN compared with SVM.

Along with accuracy, the average correct detection rate across all classes, prediction rates are often compared with two further metrics [34]. Given a specific class of interest (e.g., 'fall'), sensitivity (1), show below, is the rate of correct class detection for each class, and specificity (2), shown below, is used to measure the 'false alarm rate' of the classifier for that specific class. The average sensitivity across the 10 activities considered in this work is referred to as classification accuracy in the rest of the paper.

$$\text{Sensitivity} = \frac{\text{TruePositive}}{\text{TruePositive} + \text{FalseNegative}} \quad (1)$$

$$\text{Specificity} = \frac{\text{TrueNegative}}{\text{TruePositive} + \text{TrueNegative}}. \quad (2)$$

B. Feature Selection

Feature selection techniques improve classification accuracy and reduce computational load by removing redundant or correlated features with incorrect/confusing information [35]. These methods mainly include

- filter based methods, which are agnostic to the choice of a particular classifier and rank the different features based on information content (e.g., Euclidean distance, entropy, correlation coefficients);
- wrapper methods, which consider different combinations in the feature space and test them jointly with a specific classifier, to find the solution providing the highest accuracy. Compared to filter-based methods, wrapper methods can be resource intensive, requiring more iterations and exhaustive search, to run the classification algorithm;
- embedded methods, which integrate the classification and feature selection together with feedback (SVM-RFE) [36].

In this paper we evaluate two filter based methods, namely Fisher score (F-score) [35], Relief-F [37], and one wrapper method: sequential feature selection (SFS) [35]. F-score ranks the available features based on the distance between samples with same classes having minimal distance and different classes being a maximal distance apart. Similarly, Relief-F utilizes distance measures to give each feature a weight between -1 and 1 depending on its proximity to a certain class. SFS finds the best combinations of features by using a classifier and its accuracy as a metric to rank the features. This can be done in a forward selection by progressively adding features until the accuracy stops improving, or backwards by progressively dropping features.

Fig. 2 presents results for the SFS method for inertial sensors (accelerometer, gyroscope and magnetometer considered jointly) and the radar sensor, with a general summary for all methods provided in Table IV (inertial) and Table V (radar). Both F-score and Relief-F appear to reduce the number of features used but provide only a small 2% improvement. In terms of feature reduction for improving computational time, the optimal features suggested by filter methods were 40% and 65% of the available features for inertial sensor and radar, respectively. Classification accuracy was only boosted when SFS features were used, leading to an improvement of 5–7% in accuracy for both sensors with SVM. KNN, on the other hand, had fewer pronounced results as there was no performance improvement for the inertial sensor despite a 9% boost for radar.

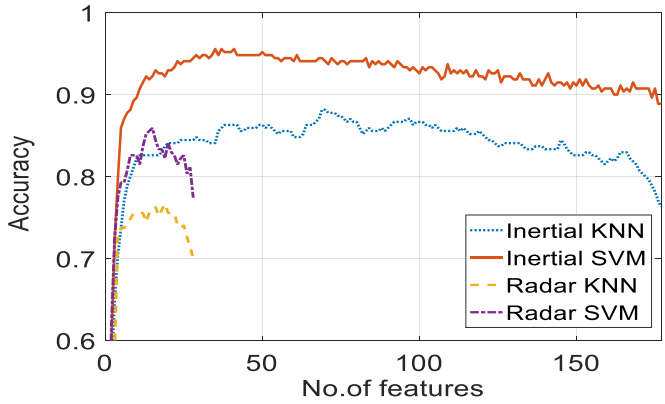

Fig. 2. Feature selection using SFS for inertial (top) and radar (bottom).

TABLE IV
COMPARISON OF FEATURE SELECTION METHODS (INERTIAL)

Method	Accuracy(%)	Time(s)	Features no.
Fscore(SVM)	90.7	1448	73
Fscore(KNN)	88.2	220.2	76
ReliefF(SVM)	91.1	1210.7	164
ReliefF(KNN)	89.3	196.9	58
SFS(SVM)	95.6	14489.5	35
SFS(KNN)	88.25	903.5	69

TABLE V
COMPARISON OF FEATURE SELECTION METHODS (RADAR)

Method	Accuracy(%)	Time(s)	Features no.
Fscore(SVM)	78.8	220.4	17
Fscore(KNN)	74.1	30.6	17
ReliefF(SVM)	74	213.1	20
ReliefF(KNN)	67	24.2	18
SFS(SVM)	85.6	1316.7	20
SFS(KNN)	79.8	32	19

Eleven most salient features were selected by the SFS algorithm for the wearable sensor, achieving over 90% accuracy; these are denoted in Tables I and II with an asterisk. Interestingly, although magnetometer performs weakly in single sensor scenario, during feature selection with inertial+radar, it appears to provide salient features, whereas physical features such as centroid and bandwidth of the spectrograms appear to be the most relevant for radar data.

V. INFORMATION FUSION METHODS

Information fusion can be used to overcome limitations of individual sensors by pooling either information or decisions from the singular sources. Fusion can be achieved at signal, feature, and decision level [36], [38], [39]. Signal level fusion can take place between sensors that record the same quantities (for example accelerometers placed on different body parts of the monitored subject), or commensurate data (e.g., accelerometer and gyroscope) that can then be combined. Feature level fusion combines in a single, larger feature vector samples generated from different sensors' data and can be followed by a feature

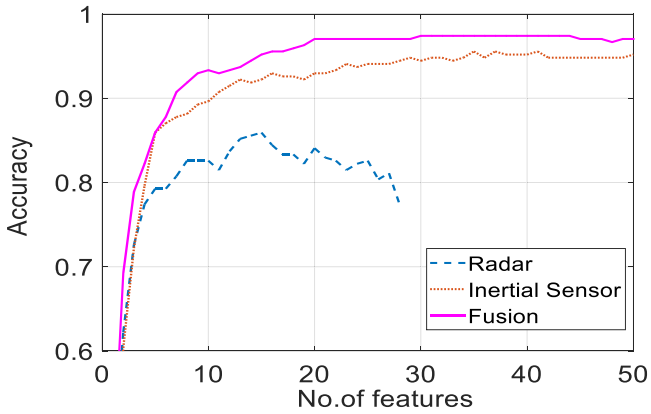

Fig. 3. Classification accuracy applying SFS to radar features, inertial features, and fusion of radar plus inertial features (SVM classifier).

TABLE VI
CONFUSION MATRIX FOR FEATURE FUSION OF DIFFERENT SENSORS WITH SFS

%	A1	A2	A3	A4	A5	A6	A7	A8	A9	A10
A1	100	0	0	0	0	0	0	0	0	0
A2	0	100	0	0	0	0	0	0	0	0
A3	0	0	100	0	0	0	0	0	0	0
A4	0	0	0	85.2	7.4	7.4	0	0	0	0
A5	0	0	0	0	92.6	3.7	0	0	3.7	0
A6	0	0	3.7	0	0	96.3	0	0	0	0
A7	0	0	0	0	0	0	100	0	0	0
A8	0	0	0	0	0	0	3.7	96.3	0	0
A9	0	0	0	0	0	0	0	0	100	0
A10	0	0	0	0	0	0	0	0	0	100

selection stage to remove redundant or incorrect features in this larger, more complex feature space. Decision level fusion is a higher level of information fusion, taking into account the predictions provided by each classifier. In this section, we present the results of feature and decision level fusion with sequential forward selection of features.

A. Feature Level Fusion

For feature level fusion, the features extracted from heterogeneous sensors were concatenated before feeding them to the classifiers. SFS is then used as feature selection method and the results are shown in Fig. 3 for a SVM classifier only, as these were found to be the best performing classifier and feature selection method. The feature combination yielding the highest accuracy includes 31 features (15% of total features), providing 97.4% classification accuracy across the 10 activities compared with previous results in Section IV, where the sole radar sensor yielded 85.6% and the homogeneous fusion of inertial sensors provided 95.6%. This improvement is 12% when compared to the results of using radar on its own, and 2% for inertial sensors on their own. However, misclassification events (highlighted in yellow), remain present between a few of the 10 activities, which is visible in Table VI as instances of "picking up object" A5 are misclassified as fall events. Despite the high classification accuracy, there is scope for improvement, which we have attempted to address by utilizing decision level fusion.

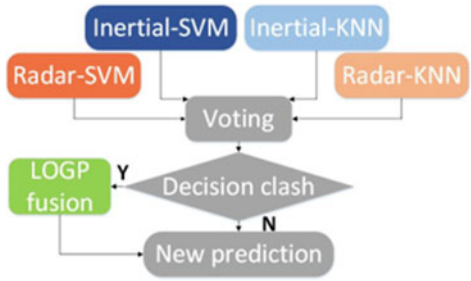

Fig. 4. Block diagram of the decision level voting system.

B. Decision Level Fusion

With this approach, the preliminary decisions of different classifiers, in the form of negated binary losses for each of the classes, are pooled. Like feature level fusion, SFS is embedded at this stage as well. The first method uses logarithmic opinion pool (LOGP) [40] and summarized in

$$B_n = e^{-S_n(c)} \tag{3}$$

$$B(\alpha|y) = \prod_{n=1}^{N} B_n(a|y)^d = \prod_{n=1}^{N} e^{-S_n(c)\,d}. \tag{4}$$

B_n is defined by a mass Gaussian function that converts the negated binary loss returned by the individual classifiers $S_n(c)$ to a posterior probability. The distribution factor d is equal to N^{-1}, where N is the number of classifiers, in this case 2. Contributions of both classifiers influence the final probability $B(\alpha|y)$, and the test sample will be assigned to the class yielding the highest probability.

The second method utilizes Fuzzy logic, where the binary loss is used as a Fuzzy set as described in (5) [36]. S_{Radar} and S_{Inertial} are two sets of negated binary loss values including 10 elements related to the 10 activities, as generated from the two SVM classifiers, whereas S_{Fused} is the new binary loss set which represents the least optimal outcome (i.e., sum of errors). The final decision is made by finding the minimal value (i.e., least errors) in this set.

$$S_{\text{Fused}}(c) = \min\{S_{\text{Radar}}(c), S_{\text{Inertial}}(c)\}. \tag{5}$$

To merge advantages from different sensors and classifiers, the third fusion algorithm is based on a novel voting system that uses predictions from two SVM and two KNN classifiers trained by inertial sensor and radar data separately, then combined for improved classification accuracy. Fig. 4 shows the voting process where each classifier predicts a class and the decision is the one supported by the majority of classifiers. In case of no clear majority (decision clash), one pass of the LOGP fusion is performed and the SVM outputs are fused to make the final prediction.

Table VII compares misclassification events and overall accuracy for the three decision fusion methods where the voting system provides the highest classification accuracy out of the decision fusion methods. Average error in Table VII indicates the average misclassification rate over the 10 iterations. The confusion matrix in Table VIII shows that false alarms for fall

TABLE VII
COMPARISON OF ACCURACY FOR DIFFERENT FUSION METHODS

Method	Average error*	Average accuracy (%)
LOGP	9	96.7
Fuzzy logic	14	94.8
Voting system	6	97.8

(*Average error is the average misclassifications over 10 iterations).

TABLE VIII
CONFUSION MATRIX FOR VOTING SYSTEM APPROACH

%	A1	A2	A3	A4	A5	A6	A7	A8	A9	A10
A1	**100**	0	0	0	0	0	0	0	0	0
A2	0	**100**	0	0	0	0	0	0	0	0
A3	0	0	**100**	0	0	0	0	0	0	0
A4	0	0	0	**88.9**	3.7	7.4	0	0	0	0
A5	0	0	0	0	**96.3**	3.7	0	0	0	0
A6	0	0	3.7	0	0	**96.3**	0	0	0	0
A7	0	0	0	0	0	0	**100**	0	0	0
A8	0	0	0	0	0	0	3.7	**96.3**	0	0
A9	0	0	0	0	0	0	0	0	**100**	0
A10	0	0	0	0	0	0	0	0	0	**100**

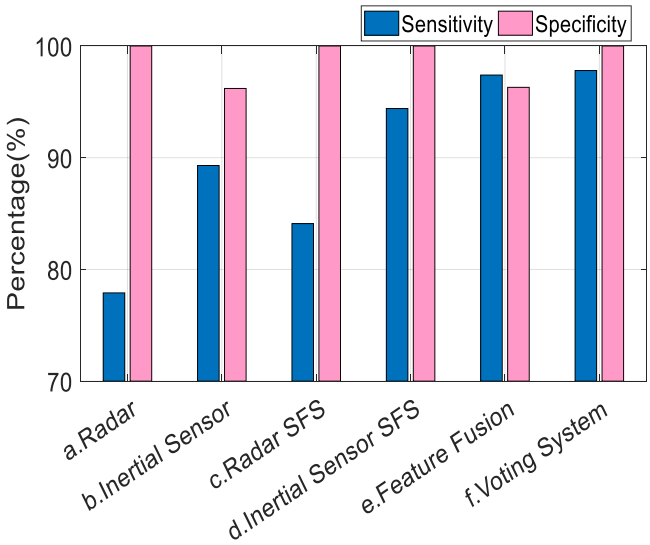

Fig. 5. Sensitivity and fall specificity for different approaches.

events have been removed, and the overall accuracy is a bit higher than in Table VI.

Fig. 5 shows a summary of specificity for fall events and average sensitivity across the 10 activities (overall classification accuracy) for all the approaches presented in this paper. A trend of progressive improvement in overall sensitivity without compromising in fall specificity can be seen by applying suitable feature selection and fusion and exploiting a combination of wearable and radar sensors information.

VI. CONCLUSION

This paper investigated the simultaneous experimental use of wearable (accelerometer, gyroscope, and magnetometer) with radar sensors, for automatic activity monitoring and fall detection in the context of assisted living. Different feature selection and information fusion techniques were presented and applied on experimental data. This can overcome the limitations in using only one sensing technology and in not considering the required diversity in features extracted from the sensors' data. Results indicated that the overall classification performance can be improved, from approximately 78–85% when using individual sensors with a large set of features, to approximately 98% when using feature level selection and multi-sensory approach and the proposed decision fusion method based on voting classifier.

Additional work will aim to collect a larger dataset to investigate different multisensory approaches, including more numerous and diverse subjects (age, body type), and different locations of the sensors (wearables on different body parts and radar with different line-of-sight to the subject). In terms of data processing, additional features can be added to the pool of those considered (e.g., "jerk" [41] or wavelet-based [19] features for wearable sensors, or additional representation domains for the radar data [42]), and additional feature selection methods and metrics for information fusion investigated. The application of deep learning methods may also be considered, in particular the challenge of using deep networks with small amount of experimental data available, for example through transfer learning approaches or through the generation of suitable simulation data. Finally, the use of multisensory approach for estimation of biomedical parameters that can have an important impact in healthcare (such as gait speed, stride length, and foot progression angle) will be also considered.

ACKNOWLEDGMENT

The authors are grateful to the many volunteers who helped with the data collection.

REFERENCES

[1] M. Terroso, N. Rosa, A. T. Marques, and R. Simoes, "Physical consequences of falls in the elderly: A literature review from 1995 to 2010," *Eur. Rev. Aging Phys. Activity*, vol. 11, no. 1, pp. 51–59, 2014.
[2] World Health Org., "WHO global report on falls prevention in older age," World Health Org., Geneva, Switzerland, 2008.
[3] U.S. Department of Health & Human Services, "Report to Congress: Aging services technology study," Washington, DC: U.S. Dept. Health Human Serv., 2012.
[4] R. M. Gibson, A. Amira, N. Ramzan, P. Casaseca-de-la-Higuera, and Z. Pervez, "Multiple comparator classifier framework for accelerometer-based fall detection and diagnostic," *Appl. Soft Comput.*, vol. 39, pp. 94–103, 2016.
[5] S. Patel, H. Park, P. Bonato, L. Chan, and M. Rodgers, "A review of wearable sensors and systems with application in rehabilitation," *J. Neuroeng. Rehabil.*, vol. 9, no. 1, 2012, Art. no. 21.
[6] J. Chen, K. Kwong, D. Chang, J. Luk, and R. Bajcsy, "Wearable sensors for reliable fall detection," in *Proc. 27th Annu. Int. Conf. Eng. Med. Biol. Soc.*, 2005, pp. 3551–3554.
[7] M. Mubashir, L. Shao, and L. Seed, "A survey on fall detection: Principles and approaches," *Neurocomputing*, vol. 100, pp. 144–152, 2013.
[8] Q. Li, J. A. Stankovic, M. A. Hanson, A. T. Barth, J. Lach, and G. Zhou, "Accurate, fast fall detection using gyroscopes and accelerometer-derived posture information," in *Proc. IEEE 6th Int. Workshop Wearable Implantable Body Sensor Netw.*, Jun. 2009, pp. 138–143.
[9] C.-C. Yang and Y.-L. Hsu, "A review of accelerometry-based wearable motion detectors for physical activity monitoring," *Sensors*, vol. 10, no. 8, pp. 7772–7788, 2010.
[10] S. J. Preece, J. Y. Goulermas, L. P. Kenney, D. Howard, K. Meijer, and R. Crompton, "Activity identification using body-mounted sensors—A review of classification techniques," *Physiol. Meas.*, vol. 30, no. 4, pp. R1–R33, 2009.

[11] K. Chaccour, R. Darazi, A. H. El Hassani, and E. Andrès, "From fall detection to fall prevention: A generic classification of fall-related systems," *IEEE Sensors J.*, vol. 17, no. 3, pp. 812–822, Feb. 2017.
[12] F. Erden, S. Velipasalar, A. Z. Alkar, and A. E. Cetin, "Sensors in assisted living: A survey of signal and image processing methods," *IEEE Signal Process. Mag.*, vol. 33, no. 2, pp. 36–44, Mar. 2016.
[13] I. H. López-Nava and A. Muñoz-Meléndez, "Wearable inertial sensors for human motion analysis: A review," *IEEE Sensors J.*, vol. 16, no. 22, pp. 7821–7834, Nov. 2016.
[14] S. C. Mukhopadhyay, "Wearable sensors for human activity monitoring: A review," *IEEE Sensors J.*, vol. 15, no. 3, pp. 1321–1330, Mar. 2015.
[15] T. R. Bennett, J. Wu, N. Kehtarnavaz, and R. Jafari, "Inertial measurement unit-based wearable computers for assisted living applications: A signal processing perspective," *IEEE Signal Process. Mag.*, vol. 33, no. 2, pp. 28–35, Mar. 2016.
[16] J. Fleming and C. Brayne, "Inability to get up after falling, subsequent time on floor, and summoning help: prospective cohort study in people over 90," *BMJ*, vol. 337, 2008, Art. no. a2227.
[17] M. G. Amin, Y. D. Zhang, F. Ahmad, and K. D. Ho, "Radar signal processing for elderly fall detection: The future for in-home monitoring," *IEEE Signal Process. Mag.*, vol. 33, no. 2, pp. 71–80, Mar. 2016.
[18] H. Li *et al.*, "Multisensory data fusion for human activities classification and fall detection," in *Proc. IEEE Sensors*, Glasgow, U.K., Oct. 29–31, 2017, pp. 909–911.
[19] C.-Y. Hsu, Y. Liu, Z. Kabelac, R. Hristov, D. Katabi, and C. Liu, "Extracting gait velocity and stride length from surrounding radio signals," in *Proc. CHI Conf. Human Factors Comput. Syst.*, 2017, pp. 2116–2126.
[20] E. Cippitelli, F. Fioranelli, E. Gambi, and S. Spinsante, "Radar and RGB-Depth sensors for fall detection: A review," *IEEE Sensors J.*, vol. 17, no. 12, pp. 3585–3604, Jun. 2017.
[21] V. C. Chen, W. J. Miceli, and D. Tahmoush, *Radar Micro-Doppler Signatures: Processing and Applications*. England, U.K.: Inst. Eng. Technol., 2014.
[22] A. Shrestha, J. Le Kernec, F. Fioranelli, E. Cippitelli, E. Gambi, and S. Spinsante, "Feature diversity for fall detection and human indoor activities classification using radar systems," in *Proc. Int. Conf. Radar Syst.*, 2017.
[23] D. Figo, P. C. Diniz, D. R. Ferreira, and J. M. Cardoso, "Preprocessing techniques for context recognition from accelerometer data," *Pers. Ubiquitous Comput.*, vol. 14, no. 7, pp. 645–662, 2010.
[24] M.-H. Lee, J. Kim, K. Kim, I. Lee, S.-H. Jee, and S.-K. Yoo, "Physical activity recognition using a single tri-axis accelerometer," in *Proc. World Congr. Eng. Comput. Sci.*, San Francisco, CA, USA, Oct. 20–22, 2009.
[25] E. Munguia Tapia, "Using machine learning for real-time activity recognition and estimation of energy expenditure," Ph.D. dissertation, Defense, Dept. Archit. Program Media Arts Sci., Massachusetts Inst. Technol., Cambridge, MA, USA, 2008.
[26] D. Tahmoush, "Review of micro-Doppler signatures," *IET Radar, Sonar Navig.*, vol. 9, no. 9, pp. 1140–1146, 2015.
[27] F. Fioranelli, M. Ritchie, and H. Griffiths, "Centroid features for classification of armed/unarmed multiple personnel using multistatic human micro-Doppler," *IET Radar, Sonar Navig.*, vol. 10, no. 9, pp. 1702–1710, 2016.
[28] A. Miller, C. Clemente, A. Robinson, D. Greig, A. Kinghorn, and J. Soraghan, "Micro-Doppler based target classification using multi-feature integration," in *Proc. IET Intell. Signal Process. Conf.*, 2013, pp. 1–6.
[29] J. De Wit, R. Harmanny, and P. Molchanov, "Radar micro-Doppler feature extraction using the singular value decomposition," in *Proc. Int. Radar Conf.*, 2014, pp. 1–6.
[30] F. Fioranelli, M. Ritchie, and H. Griffiths, "Classification of unarmed/armed personnel using the NetRAD multistatic radar for micro-Doppler and singular value decomposition features," *IEEE Geosci. Remote Sens. Lett.*, vol. 12, no. 9, pp. 1933–1937, Sep. 2015.
[31] R. Ricci and A. Balleri, "Recognition of humans based on radar micro-Doppler shape spectrum features," *IET Radar, Sonar Navig.*, vol. 9, no. 9, pp. 1216–1223, 2015.
[32] X. Shi, F. Zhou, L. Liu, B. Zhao, and Z. Zhang, "Textural feature extraction based on time–frequency spectrograms of humans and vehicles," *IET Radar, Sonar Navig.*, vol. 9, no. 9, pp. 1251–1259, 2015.
[33] T. Hastie, R. Tibshirani, and J. Friedman, *The Elements of Statistical Learning: Data Mining, Inference, and Prediction (Springer Series in Statistics),* 2nd ed. New York, NY, USA: Springer, 2009, 745 p.
[34] T. D. Bufler and R. M. Narayanan, "Radar classification of indoor targets using support vector machines," *IET Radar, Sonar Navig.*, vol. 10, no. 8, pp. 1468–1476, 2016.
[35] S. Z. Gürbüz, B. Erol, B. Çağlıyan, and B. Tekeli, "Operational assessment and adaptive selection of micro-Doppler features," *IET Radar, Sonar Navig.*, vol. 9, no. 9, pp. 1196–1204, 2015.
[36] R. C. King, E. Villeneuve, R. J. White, R. S. Sherratt, W. Holderbaum, and W. S. Harwin, "Application of data fusion techniques and technologies for wearable health monitoring," *Med. Eng. Phys.*, vol. 42, pp. 1–12, Apr. 1, 2017.
[37] R. Durgabai and Y. Ravi Bhushan, "Feature selection using ReliefF algorithm," *Int. J. Adv. Res. Comput. Commun. Eng.*, vol. 3, no. 10, pp. 8215–8218, 2014.
[38] D. L. Hall and J. Llinas, "An introduction to multisensor data fusion," *Proc. IEEE*, vol. 85, no. 1, pp. 6–23, Jan. 1997.
[39] F. Castanedo, "A review of data fusion techniques," *Sci. World J.*, vol. 2013, 2013, Art. no. 704504.
[40] C. Chen, R. Jafari, and N. Kehtarnavaz, "A real-time human action recognition system using depth and inertial sensor fusion," *IEEE Sensors J.*, vol. 16, no. 3, pp. 773–781, Feb. 2016.
[41] R. San-Segundo Zhu and J. M. Pardo, "Feature extraction for robust physical activity recognition," *Human-Centric Comput. Inf. Sci.*, vol. 7, no. 1, Dec. 2017, Art. no. 97.
[42] B. Jokanović and M. Amin, "Suitability of data representation domains in expressing human motion radar signals," *IEEE Geosci. Remote Sens. Lett.*, vol. 14, no. 12, pp. 2370–2374, Dec. 2017.

Haobo Li received the B.Eng. degree in electrical and electronic engineering from Northumbria University, Newcastle, Newcastle-upon-Tyne, U.K., and the M.Sc. degree in communication and signal processing from the University of Newcastle, in 2015 and 2016, respectively. He is currently working toward the Ph.D. degree at the School of Engineering, University of Glasgow, Glasgow, U.K. He is working on information fusion of multiple sensing technologies for assisted living applications and gesture recognition.

Aman Shrestha (S'17) received the B.Eng. degree in electronic and electrical engineering from the University of Birmingham, Birmingham, U.K. He is currently working toward the Ph.D. degree at the School of Engineering, University of Glasgow, Glasgow, U.K., working on application of radar systems and radar signal processing for assisted living, in particular activity recognition and fall detection.

Hadi Heidari (M'15–SM'17) received the Ph.D. degree in microelectronics from the University of Pavia, Pavia, Italy, in 2015. He is currently a Lecturer and Lead of the Microelectronics Laboratory, School of Engineering, University of Glasgow, Glasgow, U.K. He is a member of the IEEE Circuits and Systems Society Board of Governors, the IEEE Sensors Council Administrative Committee, and the IEEE Sensors Council Young Professional Representative. He is on the Editorial Board of *Microelectronics Journal*, a Guest Editor for the IEEE SENSORS JOURNAL, and a Guest Associate Editor for the IEEE JOURNAL OF ELECTROMAGNETICS, RF AND MICROWAVES IN MEDICINE AND BIOLOGY and IEEE Access. He was on the organizing committee of several conferences, including U.K.–China Emerging Technologies 2017 Workshop, the IEEE SENSORS'16 and '17, NGCAS'17, BioCAS'18, PRIME'15, and the organizer of several special sessions for IEEE conferences.

Julien Le Kernec (SM'17) received the B.Eng. and M.Eng. degrees in electronic engineering from Cork Institute of Technology, Cork, Ireland, in 2004 and 2006, respectively, and the Ph.D. degree in electronic engineering from the University Pierre and Marie Curie, Paris, France, in 2011. He is currently a Lecturer with the School of Engineering in the Communication, Sensing and Imaging Group, University of Glasgow, Glasgow, U.K. He held a postdoctoral position with the Kuang-Chi Institute of Advanced Technology, Shenzhen, China, from 2011 to 2012. He was a Lecturer with the Department of Electrical and Electronic Engineering, The University of Nottingham, Ningbo, China, from 2012 to 2016, prior to joining the University of Glasgow. His research interests include radar system design, software defined radio/radar, signal processing, and health applications.

Francesco Fioranelli (M'15) received the Ph.D. degree from Durham University, Durham, U.K., in 2014. He is currently a Lecturer (Assistant Professor) with the School of Engineering, University of Glasgow, Glasgow, U.K. He was a Postdoctoral Research Associate with the University College London, London, U.K., during 2014–2016, prior to joining the University of Glasgow. His research interests include development of radar systems and radar signal processing for applications including human signatures analysis for healthcare and security, drones and UAV detection and classification, automotive radar, wind farms, and sea clutter characterization. He is a Chartered Engineer through the IET and regularly acts as a Reviewer for academic journals in the domain of radar sensing, such as the IEEE TRANSACTIONS ON AEROSPACE AND ELECTRONIC SYSTEMS, the IEEE SENSORS, the IEEE TRANSACTIONS ON GEOSCIENCE AND REMOTE SENSING, and the IET Radar, Sonar and Navigation.